BIOCHEMISTRY
including biophysical chemistry & molecular biology

ARTICLE

pubs.acs.org/biochemistry

Rapid Steps in the *glmS* Ribozyme Catalytic Pathway: Cation and Ligand Requirements

Krista M. Brooks and Ken J. Hampel*

Department of Microbiology and Molecular Genetics, The Markey Center for Molecular Genetics, Stafford Hall, 95 Carrigan Drive, University of Vermont, Burlington, Vermont 05401, United States

Supporting Information

ABSTRACT: The *glmS* ribozyme is a conserved riboswitch found in numerous Gram-positive bacteria and responds to the cellular concentrations of glucosamine 6-phosphate (GlcN6P). GlcN6P binding promotes site-specific self-cleavage in the 5′ UTR of the *glmS* mRNA, resulting in downregulation of gene expression. The *glmS* ribozyme has previously been shown to lack strong cation specificity when the rate-limiting folding step of the cleavage reaction pathway is measured. This does not provide data regarding cation and ligand specificities of the *glmS* ribozyme during the rapid ligand binding chemical catalysis events. Prefolding of the ribozyme in Mg^{2+}-containing buffers effectively isolates the rapid ligand binding and catalytic events (k_{obs} > 60 min^{-1}) from rate-limiting folding (k_{obs} < 4 min^{-1}). Here we employ this experimental design to assay the cations and ligand requirements for rapid ligand binding and catalysis. We show that molar concentrations of monovalent cations are also capable of inducing the formation of the native GlcN6P binding structure but are unable to promote ligand binding and catalysis rates of >4 min^{-1}. Our data show that the sole obligatory role for divalent cations, for which there is crystallographic evidence, is coordination of the phosphate moiety of GlcN6P in the ligand-binding pocket. In further support of this hypothesis, our data show that a nonphosphorylated analogue of GlcN6P, glucosamine, is unable to promote rapid ligand binding and catalysis in the presence of divalent cations. Folding of the ribozyme is, therefore, relatively independent of cation identity, but the rapid initiation of catalysis upon the addition of ligand is stricter.

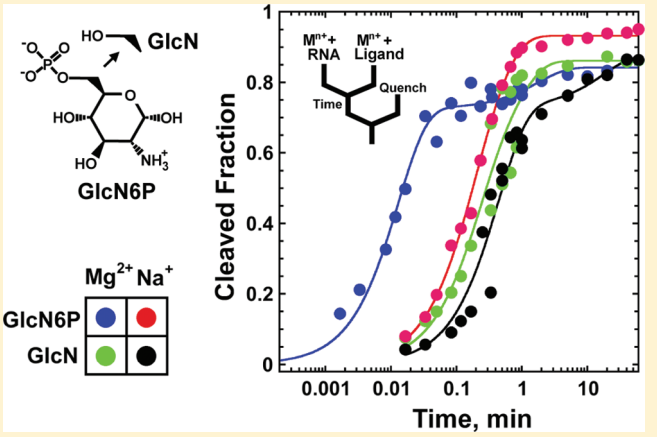

Riboswitches are structural genetic control elements that are generally located in the mRNAs that they regulate.[1−5] These motifs act as biosensors, sensitive to the intracellular concentrations of specific metabolites. The *glmS* ribozyme is a conserved riboswitch motif in numerous Gram-positive bacteria and is located upstream of the gene encoding glucosamine-6-phosphate (GlcN6P) synthetase.[6] This enzyme catalyzes the conversion of glutamine and fructose 6-phosphate to glutamate and GlcN6P, a compound that is required for sugar metabolism and cell wall biosynthesis.[6−8] Binding of GlcN6P triggers a self-cleavage reaction that results in rapid RNase J1-mediated degradation of the 3′ cleavage product, including the coding region of the mRNA.[9] Degradation of *glmS* mRNA leads to the downregulation of *glmS* protein expression, thereby decreasing the concentration of available GlcN6P. The *glmS* gene is believed to be the primary control point for cell wall synthesis in Gram-positive bacteria, including pathogenic species such as *Staphylococcus aureus*,[10] which carries a copy of the *glmS* ribozyme motif.[5]

Through the use of in-line probing,[6] X-ray crystallography,[11,12] hydroxyl radical footprinting,[13] and fluorescence resonance energy transfer (FRET),[11] it has been determined that the *glmS* ribozyme's ligand-binding pocket is preformed in the absence of its ligand.[1,11−14] In addition, we and others have determined that the ligand binding and catalysis steps can be experimentally isolated from native tertiary folding (Figure 1).[15,16] By this kinetic method, we identified a slow folding step that precedes ligand binding and catalysis.[16] Dissection of the catalytic pathway provides the opportunity to define the intrinsic base sequence and nucleotide functional group requirements as well as the extrinsic temperature, pH, and cation requirements for individual steps in the reaction pathway. In addition, experimental designs that isolate native ribozyme folding from ligand binding and catalysis open the door to a more careful examination of ligand specificity.

The ligand specificity for the *glmS* ribozyme is a significant focus of study due in large measure to the potential antibiotic use of GlcN6P analogues to disrupt cell wall synthesis in Gram-positive pathogenic bacteria. In addition, significant biochemical

Received: November 18, 2010
Revised: February 23, 2011
Published: February 25, 2011

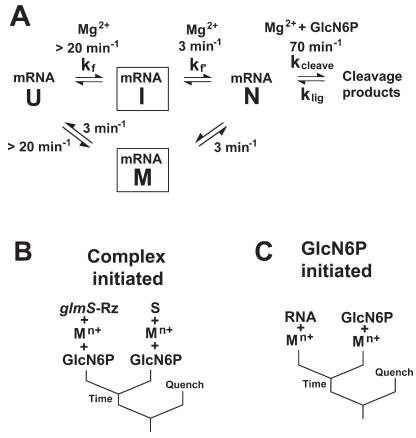

Figure 1. Folding and reaction pathway model for the *glmS* ribozyme. (A) Global folding from the unfolded (U) to a compact nativelike intermediate (I) or misfolded (M) form occurs rapidly upon addition of $MgCl_2$. A second Mg^{2+}-dependent event folds the catalytic RNA into a complex capable of GlcN6P binding (N). GlcN6P binding and catalysis occur on a second time scale once the native (N) structure is formed. (B) A complex-initiated experimental design assays the rate of formation of N. (C) Ligand binding and catalysis can be assayed in a manner independent of the rate-limiting step by prefolding *glmS*-Rz-S in cations and triggering reactions through the addition of ligand.

and structural data point to the hypothesis that the ligand functions as a coenzyme in the *glmS* reaction.[12,14,17,18] The amine residue of GlcN6P is in a position to serve as a proton donor to the G + 1 5′ oxygen. This function is unique among naturally occurring ribozymes and has an impact on our understanding of the enzymatic repertoire of ribozymes because coenzymes provide numerous chemical functionalities not present in RNA.[19] Crystallographic data support a ligand binding model in which the GlcN6P makes contacts with Mg^{2+} ions and RNA. Two fully hydrated Mg^{2+} ions can be modeled into the ligand-binding pocket and are hypothesized to make a set of water- and outer sphere-mediated contacts that bridge the phosphate group of GlcN6P and RNA functional groups. Although present in the catalytic core, these Mg^{2+} ions are not in a position to directly participate in reaction chemistry.[12,17,20] In addition, phosphorothioate substitution within the catalytic core of the *Bacillus cereus glmS* ribozyme was rescued by Mn^{2+} at sites that mediate ligand phosphate recognition.[20] Protonation of the ligand phosphate is expected to have a negative impact on binding by altering this network of Mg^{2+} and water interactions and has been proposed to give rise to an increase in GlcN6P binding affinity as a function of pH.[15] In addition, a hydrogen bonding interaction between a GlcN6P phosphate oxygen and the N1 hydrogen of the highly conserved G1 residue has been proposed.[21] Substitution of G1 with adenosine has a large impact on GlcN6P-mediated cleavage activity but only a modest effect on activity in the presence of a nonphosphorylated ligand analogue glucosamine, GlcN. Because most experiments that have specifically addressed the question of ligand specificity have utilized protocols that do not rule out the impact of slow global folding on their outcome, we have an incomplete picture of the requirements for the very rapid ligand binding that has been observed in the *glmS* system. Finally, the degree to which divalent cations are required for rapid ligand binding and ligand specificity has not been specifically addressed.

Cations play important roles in the formation of ribozyme tertiary structure and can participate directly in catalysis.[22,23] In some cases, ribozymes that were previously thought to function as metalloenzymes have been found to work well in the absence of cations capable of assisting in active site catalysis.[24,25] In addition, the *Thermotoga maritima* lysine riboswitch has been shown to form nearly identical structures in the presence of K^+ and Mg^{2+} ions.[26] In many ribozyme systems, high concentrations of monovalent cations can support significant activity.[27−30] In most cases, however, monovalent cation-supported activities are lower than those obtained in divalent cations. These differences have been ascribed to divalent cations, notably Mg^{2+}, being uniquely suited to assist directly in chemical catalysis as seen in group I and II introns,[31−33] and guiding the formation of specific tertiary structures required for optimal catalysis.[34] These types of experiments are important because they have the potential to define the obligatory roles for specific types of cations in the function of catalytic RNAs. A general lack of cation specificity for catalysis has been observed for the *glmS* ribozyme. Monovalent cations, several divalent cations, and cobalt hexaammine have all been shown to allow for some level of activity. These experiments, however, followed the rate-limiting step in the reaction pathway.[6,17,35] Therefore, in the presence of cations that permit rapid ligand binding, these data probably represent the rate of formation of the native ribozyme structure or unfolding of a non-native intermediate rather than the rate of ligand binding and catalysis. We know little about the range of cations that are able to support rapid ligand binding and catalytic activity that we and others have observed.

Here we present a ribozyme kinetics study aimed at defining the cation and ligand requirements for fast catalysis by the *glmS* ribozyme. Our data support the hypothesis that the ligand phosphate is involved in rapid binding and that divalent cations are uniquely suited to provide a rapid GlcN6P binding mode. In addition, we have observed that the *glmS* ribozyme, folded in the presence of monovalent cations, is indistinguishable from one folded in Mg^{2+}.

EXPERIMENTAL PROCEDURES

RNA Preparation. The 19-nucleotide substrate RNA (Figure 2A) was generated on an Applied Biosystems DNA/RNA synthesizer using standard phophoramidite chemistry from Glen Research. The RNA products were deprotected and purified by denaturing PAGE and reverse phase HPLC as described previously.[36] The *glmS*-Rz and *glmS* 3′ P RNAs (Figure 2) were made by transcription of double-stranded DNA templates with T7 RNA polymerase. Transcription templates were constructed by annealing two large overlapping DNAs, filling the single-stranded regions with Klenow fragment DNA polymerase, and subsequent PCR amplification as previously described.[13] To generate *glmS*-3′ P cleavage products, 10 mM GlcN6P was added to *glmS*-cis transcriptions following the standard transcription incubation of 3 h, and this mixture was allowed to incubate for an additional 1 h at 37 °C. All transcription products were purified by polyacrylamide gel electrophoresis as described previously.[37] Radiolabeled RNAs were prepared by phosphorylation of the 5′-terminal hydroxyl with [γ-^{32}P]ATP (ICN) and polynucleotide kinase.

Ribozyme Cleavage Kinetics. A 25 mM TAPS/HEPES/cacodylate/sodium acetate (THCA) buffer was utilized as previously described at all pH values so that buffer-specific effects could be minimized.[16] All buffer reagents were purchased from Sigma. The pH of THCA was adjusted via addition of NaOH to

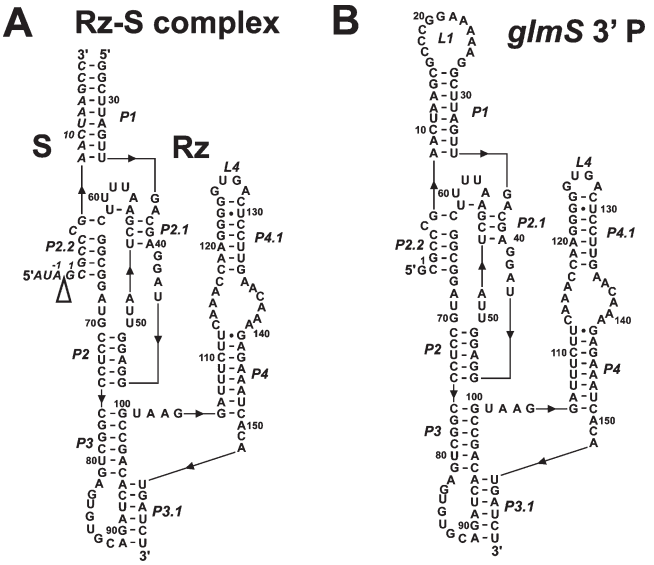

Figure 2. Secondary structure diagrams of the *Bacillus subtilis glmS* trans-acting ribozyme−substrate complex (*glmS*-Rz-S) used in cleavage kinetics experiments (A) and *glmS* 3′ cleavage product (B) used in hydroxyl radical footprinting. The secondary structures are shown according to existing crystal structures for the *glmS* ribozyme[12,14] and numbered according the system of Winkler and co-workers.[6] The 5′ to 3′ direction of the RNA is indicated with black triangles. The cleavage site is denoted with an empty triangle.

each buffer stock. The final concentration of Na^+ ions was, therefore, different at each pH. This difference was adjusted by the addition of NaCl to reaction buffers at pH >6 so that the final concentration of Na^+ was equal to 60 mM for all reaction mixtures. The pH of ligand stocks were adjusted to the pH of the reaction mixture to which they were added. All RNAs were subjected to a 2 min incubation at 70 °C in 25 mM THCA with 0.1 mM EDTA followed by a 5 min benchtop cooling time. This incubation served to release the RNAs from any nonproductive conformations present upon thawing. All ribozyme kinetics assays were single-turnover experiments in which the concentration of *glmS*-Rz was 0.5 μM and labeled substrate was present at a concentration of <10 nM. The reaction time course were generally continued for 7 h for reaction rates of <0.1 min^{-1} and 1 h for reaction rates of >0.1 min^{-1}.

Complex-Initiated Reactions. RNAs were incubated in 25 mM THCA (pH 7.5) in the presence of various mono-, di-, and multivalent cations and 15 mM ligand at 25 °C for 1.5 h. Cleavage reactions were initiated via addition of an equal volume of a solution containing 25 mM THCA and specified concentrations of *glmS*-Rz, cation, and GlcN6P. Reactions were quenched via addition of 1 μL of the reaction mixture to 9 μL of loading buffer, 95% (v/v) formamide, 25 mM EDTA, 0.01% (w/v) bromophenol blue, and 0.01% (w/v) xylene cyanol. Reactions performed in 3 M NaCl were quenched via addition of 1 μL of the reaction mixture to 49 μL of loading buffer. The reaction products were separated on denaturing 20% polyacrylamide gels, and the data were quantified using Bio-Rad phosphorimager analysis and Quantity One 1-D. The resulting data points were plotted and fitted using Synergy's Kalidegraph (version 3.6) to the double-exponential equation $y = y_o = A_1(1 - e^{-t/\tau_1}) + A_2(1 - e^{-t/\tau_1})$, yielding cleavage rate constants k_i $(=1/\tau_1)$ and amplitudes A_i. Rapid quench reactions were conducted on a three-syringe Kintek rapid quench mixer. Equal volumes from the two sample ports containing RNA and buffer components as described were pushed into the mixing chamber to initiate reactions. The push buffers were identical in composition to the samples that they pushed without the RNA and GlcN6P. The quench syringe contained rapid quench buffer (RQB), 86% (v/v) formamide, 35 mM EDTA, and 1× Tris-borate-EDTA (TBE) buffer. Reaction mixtures containing a monovalent cation background were expelled into microcentrifuge tubes containing 400 μL of additional RQB, as listed above.

Ligand-Initiated Reactions. RNAs were incubated in 25 mM THCA, pH 7.5, in the presence of 3 M NaCl and 1 mM EDTA and incubated at 25 °C for 1.5 h. Cleavage reactions were initiated via addition of an equal volume of a solution containing 25 mM THCA and specified concentrations of cation and GlcN6P. Reactions were quenched via addition of 1 μL of the reaction mixture to 49 μL of loading buffer, 95% (v/v) formamide, 25 mM EDTA, 0.01% (w/v) bromophenol blue, and 0.01% (w/v) xylene cyanol. The reaction products were separated on denaturing 20% polyacrylamide gels, and the data were quantified and fit as described above. Rapid quench reactions were conducted as described above and quenched into 400 μL of additional RQB as described above.

Measurement of the Rate of GlcN6P-Independent Folding. Unlabeled ribozyme and 5′-end-labeled substrate were incubated separately in 25 mM THCA in the presence of 15 mM $MgCl_2$ for 1.5 h at 25 °C. Folding reactions were initiated via addition of equal volumes of ribozyme and substrate solutions together. At various time points a 15 mM GlcN6P, chase was added to the reaction mixture, and the mixture was incubated for 5 s before the reaction was quenched. Time points faster than 10 s reactions were conducted on a three-syringe Kintek rapid quench mixer. The right sample syringe contained 5′-end-labeled cleavable substrate in 25 mM THCA (pH 7.5) and 15 mM $MgCl_2$. The left sample syringe contained cold ribozyme in the presence of 25 mM THCA (pH 7.5) and 15 mM $MgCl_2$. Buffer syringes contained 25 mM THCA and 15 mM $MgCl_2$. The quench syringe contained equal concentrations of buffer and Mg^{2+} in addition to saturating concentrations of GlcN6P. Individual reactions proceeded with an initial mixing of equal volumes of the two sample syringes. This mixture was allowed to fold for a specified time at 25 °C prior to being rapidly mixed with GlcN6P from the quench syringe. When the quench syringe solution is introduced into the reaction mixture, GlcN6P binds the native Rz-S complex, resulting in cleavage of the RNA backbone. This solution is pushed into an empty microcentrifuge tube and allowed to incubate for 5 s, and then the reaction is quenched with 400 μL of RQB. Substrate and product were separated on 20% denaturing polyacrylamide gels and analyzed with a Bio-Rad phosphorimager as described above.

pH Dependence of Ligand-Initiated Reactions. RNAs were incubated in 25 mM THCA, pH 5.5 to pH 8, in the presence of 15 mM $MgCl_2$ or 3 M NaCl and 1 mM EDTA at 25 °C for 1.5 h. Cleavage reactions were initiated via addition of an equal volume of a solution containing 25 mM THCA and specified concentrations of cation and saturating concentrations of either GlcN6P or GlcN (Figures S3 and S4 of the Supporting Information). Reactions including $MgCl_2$ were quenched via addition of 1 μL of the reaction mixture to 9 μL of loading buffer, 95% (v/v) formamide, 25 mM EDTA, 0.01% (w/v) bromophenol blue, and 0.01% (w/v) xylene cyanol. Reactions including a 3 M NaCl background were quenched via addition of 1 μL of the reaction mixture to 49 μL

of loading buffer. The reaction products were separated on denaturing 20% polyacrylamide gels, and the individual cleavage rates were quantified and fit using the double-exponential equation described above. Cleavage rates were plotted as a function of pH and fit to the single-ionization equation $k_{obs} = k_{max}/(1 + 10^{pK_a - pH})$, where k_{max} is the intrinsic rate of the cleavage reaction and pK_a is the acid dissociation constant of a single titrating functional group. Rapid quench reactions were conducted as described above, and reactions including 3 M NaCl were additionally quenched into 400 μL of RQB, as described above.

Equilibrium Hydroxyl Radical Footprinting Reactions. End-labeled *glmS* 3′ cleavage product (Figure 2A) was incubated in a buffer containing 25 mM sodium cacodylate (pH 7) and a range of NaCl and $MgCl_2$ concentrations for 2 min at 70 °C followed by 90 min at room temperature and then probed using hydroxyl radicals as described previously.[13] Polyacrylamide gel electrophoretic separation of the cleavage products and quantification of the results were conducted according to our previously published methods.[13] Protected fractions at each site were normalized to the highest level of protection observed in individual experiments and plotted as a function of cation concentration. Magnitudes of protection matched our previously reported range.[13]

RESULTS

Our objective for this work was to define the cation specificity and ligand requirements for the rapid ligand binding and catalysis that we and others have observed upon addition of ligand to prefolded ribozymes (Figure 1).[15,16] We have previously demonstrated that the *glmS* ribozyme rapidly collapses into a nearly native tertiary structure as shown by time-resolved hydroxyl radical footprinting.[16] These experiments, performed in the presence and absence of GlcN6P, indicate a rapid compaction ($\sim$1 s^{-1}) of the ribozyme into a (nearly) native tertiary structure without any evidence of a distinct conformational rearrangement. In contrast, the *glmS* ribozyme achieves a catalytically active conformation on a much slower time scale, $\sim$3 min^{-1}, in the presence of saturating levels of $MgCl_2$ and GlcN6P. This slow step is cation-dependent and must be completed prior to catalysis (Figure 1A). These experiments were performed in the presence of GlcN6P and, therefore, do not provide data for the potential of ligand-induced behavior during this transition. Therefore, before examining the requirements for rapid ligand binding and catalysis, we wanted to be able to rule out ligand-assisted prefolding of the native complex.

To monitor the rate-limiting folding event in the absence of ligand, we performed "GlcN6P chase" experiments. Briefly, trans-ribozyme−substrate complex [*glmS*-Rz-S (Figure 2A)] was prefolded in $MgCl_2$ in the absence of GlcN6P for varying amounts of time. After this folding time, we introduced a saturating concentration of GlcN6P into the solution and allowed the reaction to proceed for 5 s before quenching (Figure 3A). The 5 s chase time was chosen for these reactions because of the observation that when the ribozyme−substrate complex was folded in $MgCl_2$-containing solutions prior to initiation via addition of a saturating concentration of GlcN6P, >80% substrates are cleaved during this time.[16] In addition, the 5 s chase time can be accurately and reproducibly made by hand mixing. Although cation-dependent folding is ongoing during the short chase time, we did not expect this to significantly increase the apparent rate of this slow step in the reaction. Thus, we measured the fraction of molecules that are folded into a catalytically active conformation as a function of folding time. Experiments were performed in the rapid quench and via hand-held mixing. We observed equal global folding rates, within error, in the presence and absence of GlcN6P [3.5 ± 0.1 and 3.4 ± 0.26 min^{-1}, respectively (Figure 3B)]. These findings support our previous data indicating that the rate-limiting step is cation-dependent with no detectable influence of GlcN6P. We have also demonstrated, through the use of two distinct experimental designs, that the ligand binding and catalysis steps of the reaction pathway can be isolated from this slow, rate-limiting, folding step by preincubating the RNA in $MgCl_2$ prior to initiation of catalysis (Figure 1).[16]

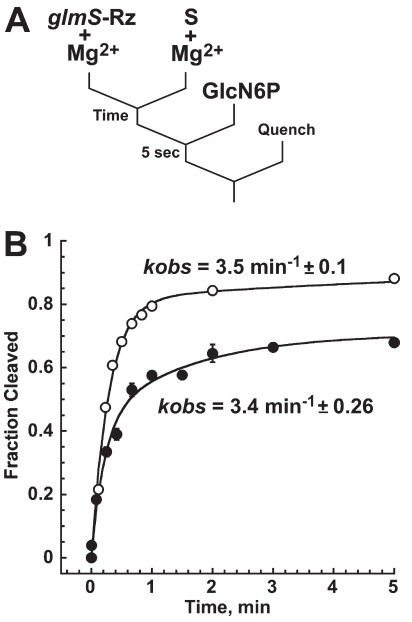

Figure 3. Determining the global folding rate of the *glmS* ribozyme in the absence of GlcN6P. (A) Experimental design used to determine the rate of global folding in the absence of GlcN6P. Ribozyme and substrate strands were mixed in the presence of $MgCl_2$ and allowed to fold for a specific time. The level of native folding was then assayed by addition of GlcN6P for a fixed period of time, 5 s. (B) Comparison of a representative complex-initiated reaction (○) in the presence of GlcN6P previously reported[16] and three replicate GlcN6P chase reactions (●) (error bars set at one standard deviation). The fraction of substrate cleaved is plotted as a function of time and fit to a double-exponential equation as described in Experimental Procedures.

To gain a better understanding of the cation specificity of the *glmS* ribozyme, we sought to elucidate the role that cations play in the process of folding, ligand binding, and catalysis. We utilized the *glmS*-Rz-S construct (Figure 2B) and performed single-turnover kinetic complex-initiated experiments, as previously described[16] (Figure 1B) in the presence of mono-, di-, and multivalent cations. This assay measures the rate-limiting step of the catalytic pathway. Our findings support previous data showing a lack of strong cation specificity as measured in this manner.[17] Mn^{2+} and Ca^{2+} ions promote rates of self-cleavage that are similar (within a 4-fold range) to those in the presence of Mg^{2+} (Figure 4 and Table 1). $Co(NH_3)_6^{3+}$, an exchange-inert structural mimic of hexahydrated Mg^{2+}, associates with RNA only through outer sphere and electrostatic interactions.[38] This cation promotes a cleavage rate 1 order of magnitude slower than that achieved in $MgCl_2$. In addition, we

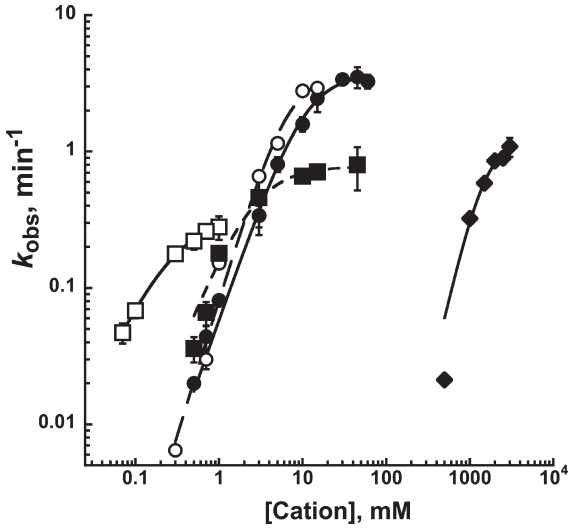

Figure 4. Complex-initiated trans-cleavage reactions in various cations. Complex-initiated cleavage assays were conducted as described previously,[16] utilizing the *glmS*-Rz-S construct, at pH 7.5. Experiments were conducted over a range of cation concentrations using saturating amounts of GlcN6P. Reaction rates were plotted as a function of cation concentration on a log scale. The symbols used for each cation are shown in the graph: Mg^{2+} (●), Ca^{2+} (○), Mn^{2+} (■), $Co(NH_3)_6^{3+}$ (□), and Na^+ (◆). All data points are the average of three replicate experiments with error bars set at one standard deviation from the mean. Individual titrations were fit to the Hill equation as described in Experimental Procedures. k_{obs}^{max}, K_d^{app}, and the Hill cofficient, *n*, for each cation are reported in Table 1.

Table 1. Apparent K_d Values and Maximal Cleavage Rates (k_{obs}^{max}) for Complex-Initiated Reactions[a] Employing a Variety of Cations at pH 7.5

cation	K_d^{app}[b]	k_{obs}^{max} (min^{-1})	*n*
Na^+	1.5 M	1.2	2.7
Mg^{2+}	10 mM	3.6	2.0
Ca^{2+}	6 mM	3.4	2.5
Mn^{2+}	2.5 mM	0.77	1.5
$Co(NH_3)_6^{3+}$	0.28 mM	0.33	1.3

[a] The complex-initiated experimental design is outlined in Figure 1B and described in Experimental Procedures. [b] K_d values were determined by fitting k_{obs} vs cation concentration plots to the Hill equation, as described in Experimental Procedures, where the value for the Hill coefficient (*n*) is shown above for each cation tested.

observed that the use of molar concentrations of NaCl resulted in cleavage rates within 3-fold of the rate achieved in $MgCl_2$ (Figure 4).[17] These data support previous findings indicating the *glmS* ribozyme lacks an essential role for divalent metal ions in either the folding process or the promotion of catalysis.[17] K^+ ions have been found to promote catalysis at rates similar to molar concentrations of Na^+ ions.[17] Next, we wanted to determine if molar concentrations of NaCl are sufficient to fold the *glmS* motif into its native tertiary structure. Equilibrium hydroxyl radical footprinting experiments were performed using the *glmS* 3′-cleavage product (Figure 2B) in increasing concentrations of NaCl. Figure 5 shows the comparison solvent protection as a function of NaCl concentration and 15 mM $MgCl_2$ at two sites on the ribozyme backbone. A12 is protected by a long-range tertiary interaction between the L4 tetraloop and P1

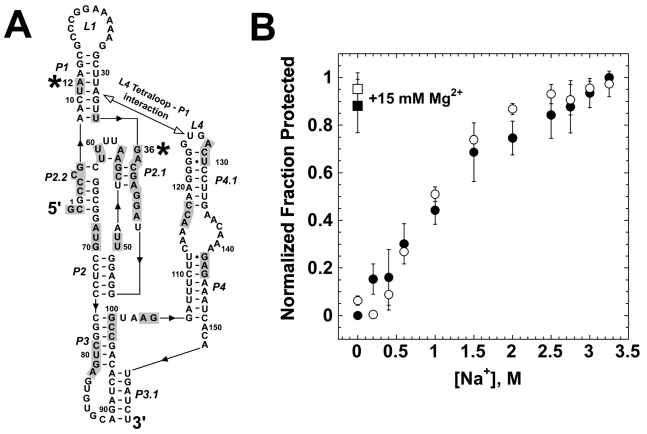

Figure 5. Global folding of the *glmS*-3′ P as a function of Na^+ concentration. End-labeled *glmS*-3′ P was folded at the indicated concentration of Na^+ or 15 mM Mg^{2+} and then probed with hydroxyl radical as described in Experimental Procedures. (A) Secondary structure of *glmS*-3′ P with the sites of hydroxyl radical protection shaded. Positions 12 and 36 are denoted with asterisks. (B) Quantification of the solvent protection at one site of the core tertiary structure, G36 (empty symbols), and one site of peripheral tertiary interaction, A12 (filled symbols), in the presence of 15 mM $MgCl_2$ (squares) and a range of NaCl concentrations (circles).

(Figure 2). G36 is protected by formation of the core double-pseudoknot structure.[14] The results from the quantification of these two sites are representative of the entire protection pattern in molar NaCl and 15 mM $MgCl_2$. These experiments revealed that molar concentrations of Na^+ ions are sufficient to promote equivalent solvent protection at the same RNA sites as obtained in the presence of $MgCl_2$ (Figure 5 and Figure S1 of Supporting Information).

Because molar concentrations of NaCl are capable of prefolding a native tertiary structure, we sought to determine if 3 M NaCl could promote rapid ligand binding and chemical catalysis in a GlcN6P-initiated experimental design (Figure 1C). Briefly, the ribozyme and substrate were preincubated together in 3 M NaCl for 90 min. This time of incubation is sufficient to allow Rz-S complexes to reach a prefolded equilibrium end point. Reactions were then initiated by the addition of a saturating concentration of GlcN6P in the presence or absence of 15 mM $MgCl_2$. The background concentration of NaCl was maintained at 3 M for the initiation of the reactions. To ensure saturation of the system with GlcN6P in a background of 3 M NaCl, a shallow titration of ligand was conducted using a 3 M NaCl background to prefold the ribozyme−substrate complex and various cations and GlcN6P to initiate the reaction (see Figure S3 of the Supporting Information). Little variation in the concentration of ligand required to saturate the reaction among the various cations was observed in these experiments. We compared the results of experiments performed in 3 M NaCl, with or without 15 mM $MgCl_2$, with the results of identical experiments in which prefolding and GlcN6P initiation were conducted in 15 mM $MgCl_2$ (Figure 6A). Reactions initiated with GlcN6P in 3 M NaCl and 15 mM $MgCl_2$ proceeded with the same rate as reactions initiated with GlcN6P and 15 mM $MgCl_2$ (Figure 6A). However, reactions that were initiated in the presence of 3 M NaCl as the sole cation proceeded 18-fold slower than those initiated in the presence of 15 mM $MgCl_2$ (Figure 6A). These findings indicate that molar concentrations of monovalent cations are sufficient to induce the formation of the native coenzyme

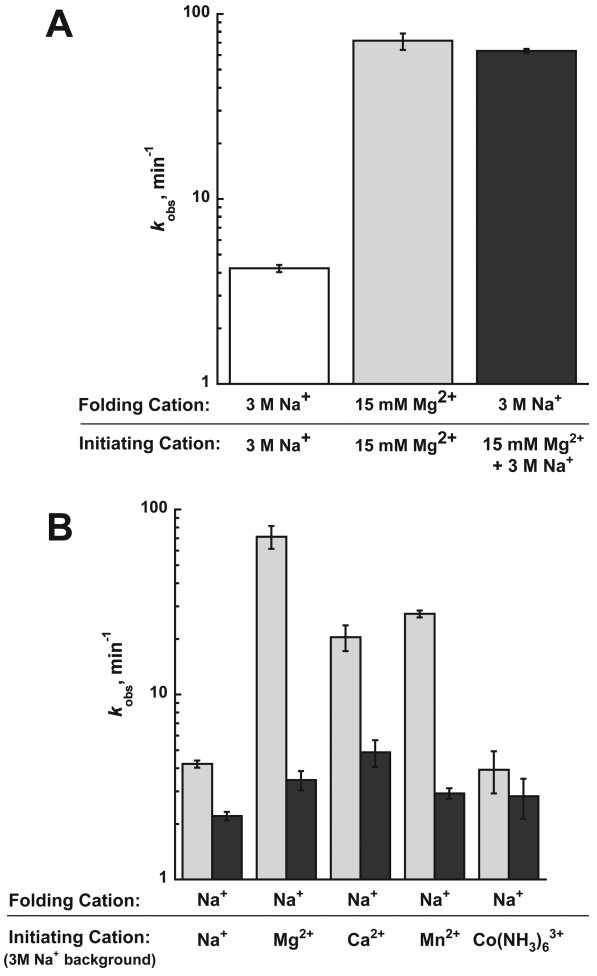

Figure 6. GlcN6P-initiated trans-cleavage demonstrates the requirement for both divalent cations and a ligand phosphate for fast catalysis. GlcN6P-initiated cleavage reactions were conducted at pH 7.5, utilizing the *glmS*-Rz-S construct as described previously.[16] (A) Reaction rates determined as described in Experimental Procedures plotted as a function of the folding and initiating cations, 15 mM $MgCl_2$ and 3 M NaCl, respectively, in the presence of saturating concentrations of GlcN6P. (B) Loss of rapid cleavage kinetics in the absence of the ligand phosphate group. Reactions were initiated using various cations and saturating levels of GlcN6P (empty bars) or GlcN (filled bars) after prefolding *glmS*-Rz-S in 3 M NaCl for 90 min. The following concentrations of cations were used: 15 mM $MgCl_2$, $CaCl_2$, and $MnCl_2$; 10 mM $Co(NH_3)_6^{3+}$; and 3 M NaCl (maintained in a buffer containing 3 M NaCl). All reaction rates are the average of three replicate experiments, and error bars indicate one standard deviation from the mean.

binding structure but do not result in the rapid burst of catalysis in the presence of GlcN6P (Figure 6A). Overall, our data suggest that the ribozyme−substrate complex can be prefolded in 3 M NaCl into a native structure equivalent to that produced in $MgCl_2$.

Having previously demonstrated a lack of cation specificity through the slow folding step of the reaction pathway (Figure 4), we wanted to explore the ability of a variety of cations to promote fast ligand binding and reaction chemistry. To do this, we utilized the ability of the ribozyme to fold to a native ligand-unbound, or apo, conformation in 3 M NaCl. Reactions were initiated with saturating concentrations of both GlcN6P and the cations listed while maintaining 3 M NaCl (Figure 6B, empty bars). Our data show that the identity of the cation affects the ability of the *glmS* ribozyme to undergo rapid catalysis in a background of monovalent cation. Of the divalent cations tested, Mg^{2+} was most efficient in promoting rapid catalysis in the presence of ligand, with Mn^{2+} and Ca^{2+} promoting similar catalytic rates under these conditions (Figure 6B). The reduced catalytic rate in the presence of Mn^{2+} and Ca^{2+} ions could be the result of conformational or structural limitations of the active site. Although Mn^{2+} and Ca^{2+} are the smallest and largest of the divalent cations tested, at 0.67 and 1.12 Å, respectively, they exhibit essentially no difference in their ability to promote catalysis in the presence of ligand. These data suggest an optimal cation size necessary to effectively position the ligand and promote catalysis.[39] $Co(NH_3)_6^{3+}$, a structural analogue of fully hydrated Mg^{2+}, was very inefficient at promoting catalysis in the presence of ligand, with a cleavage rate that was only slightly higher than the rate of cleavage triggered by ligand and 3 M NaCl alone (Figure 6B). Unlike the associated water ligands of Mg^{2+}, Ca^{2+}, and Mn^{2+}, the ammine ligands of $Co(NH_3)_6^{3+}$ cannot be displaced to make inner sphere contacts.[38] This indicates that to achieve rapid catalysis, there may be a requirement for water-mediated coordination to achieve appropriate or rapid placement of GlcN6P within the binding pocket. Overall, our data suggest that divalent cations are more effective than monovalents or $Co(NH_3)_6^{3+}$ at positioning GlcN6P within the ligand-binding pocket. Alternatively, $Co(NH_3)_6^{3+}$ may induce ribozyme conformation that is not optimal for rapid catalysis.

Crystallographic structures indicate the presence of two fully hydrated magnesium ions within the ligand-binding pocket of the *glmS* ribozyme.[12] The magnesium ions coordinate the phosphate group of GlcN6P in addition to making contacts with the RNA backbone and multiple functional groups within the active site. To test the hypothesis that rapid ligand binding and catalysis are assessed in part by interactions between Mg^{2+} and the ligand phosphate, we examined the ability of glucosamine (GlcN), a nonphosphorylated analogue, to promote ligand-initiated reactions. Substitution of GlcN for GlcN6P largely eliminates the cation-dependent variability in ligand-initiated cleavage rates observed with GlcN6P (Figure 6B). Indeed, all GlcN-initiated reactions rates are within approximately 2-fold of one another and are all below 4.5 min^{-1}. It should be noted that under all conditions we have employed GlcN at a concentration beyond which we see no further rate enhancement (see Figures S3 and S4 of the Supporting Information). These data support the hypothesis that an interaction between divalent cations and the phosphate moiety of GlcN6P increases the ligand binding rate.

In addition to interacting with the phosphate group of GlcN6P, crystallographic structures also show the Mg^{2+} ions making contact with nucleobase functional groups within the ligand-binding pocket. Additionally, previous experiments have shown that GlcN6P binding is weak at low pH, which has been postulated to be due to neutralization of the phosphate moiety and loss of the ability to coordinate Mg^{2+}.[15] The pK_a of the phosphate group has been determined, via NMR, to be ~6.1.[15] To examine the possibility of Mg^{2+}-dependent pH effects, we determined the rate−pH profiles of GlcN6P-initiated reactions in $MgCl_2$ and 3 M NaCl (Figure 7). When the reaction is triggered with $MgCl_2$ and GlcN6P, we observed a base activation rate−pH profile with a k_{max} of 70 and a pK_a of 6.2 when fitting to an equation assuming a single titratable group (Figure 7). The pK_a for this experiment is very close to previous findings[15] (Figure 7). Reactions initiated with 3 M NaCl and GlcN6P display a pK_a of 6.4 and also fit to an equation assuming a single

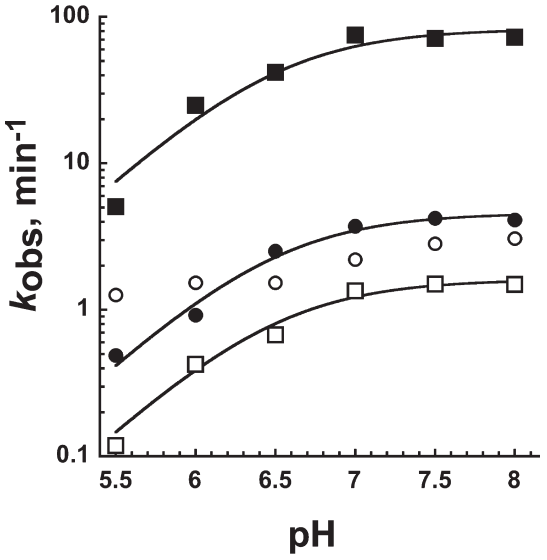

Figure 7. pH dependence of *glmS* ribozyme trans-cleavage in the presence of GlcN6P or GlcN. Reaction rates determined as described in Experimental Procedures are plotted as a function of pH (pH 5.5−8). The *glmS*-Rz-S construct was prefolded in $MgCl_2$ (squares) or 3 M NaCl (circles) for 90 min prior to initiation of the reaction with saturating concentrations (see Figure S4 of the Supporting Information) of GlcN6P (filled symbols) or GlcN (empty symbols). The data were fit to a single-ionization equation as described in Experimental Procedures. Each data point is the average of three replicate experiments, and error bars indicating one standard deviation from the mean are shown but are smaller than the symbols.

titratable group, but with an 18-fold lower k_{max}. When the same reactions were initiated with GlcN, we observed the same pH-dependent reactions in the presence of $MgCl_2$ but not NaCl. In 3 M NaCl, GlcN-initiated reactions displayed an only 2-fold increase in the cleavage rate over the pH range of 5.5−8 (Figure 7). These data indicate that removal of the phosphate moiety in the presence of Mg^{2+} ions does not eliminate the pH dependence of the catalytic reaction, as observed with Na^+ as the sole cation.

DISCUSSION

The rate of the *glmS* ribozyme reaction pathway is limited by a slow folding step that precedes formation of a native structure capable of ligand binding.[16] Having previously shown that the pathway can be dissected such that the combined rate of the ligand binding and catalysis steps can be studied in isolation from this rate-limiting step, our goal in this work was to define the cation and ligand requirements for these rapid steps.[16] All previous examinations of the cation requirements for the *glmS* ribozyme have used experimental designs that assay the rate-limiting step in the pathway.[6,17] Here we have shown that in molar concentrations of Na^+ ions, the ribozyme is able to fold to the native state and catalyze reactions through the rate-limiting step at a rate similar to that observed in $MgCl_2$-containing solutions (Figures 4 and 5). We define "through the rate-limiting step" as complex-initiated reactions in which the ribozyme−substrate complex must fold into its native three-dimensional structure during the assay. More importantly, a high NaCl concentration allows the ribozyme to fold into a complex that is competent to bind ligand, preincubated in $MgCl_2$, rapidly ($\geq$70 min^{-1}) and execute chemical catalysis (Figure 6A). These data also indicate that the reduction in water activity in 3 M NaCl compared to dilute salt conditions does not strongly influence the folding of the ribozyme (Figure 5). We cannot exclude the possibility that this solution property plays a role in the low catalytic rate of the glmS ribozyme in 3 M NaCl. However, our data fit more closely to a model in which Mg^{2+} ions are particularly well suited to the promotion of rapid ligand binding and catalysis.

Molar concentrations of monovalent cations, such as Na^+, K^+, Li^+, and NH^{4+}, have been employed in a number of ribozyme systems in defining the specific requirements for Mg^{2+} in ribozyme structure and catalysis.[22,40,41] Though molar concentrations of monovalents are not physiological, they can serve to define structural and catalytic roles uniquely suited to divalent cations.[28,30,42] We have observed Na^+-mediated native folding of the *glmS* ribozyme into a tertiary structure that is able to bind GlcN6P and Mg^{2+}, without any apparent conformational change, and direct catalysis very rapidly. This suggests that the sole obligatory role for Mg^{2+} ions in the *glmS* system is to assist in ligand binding. We are limited in this interpretation in one respect only. If a Mg^{2+}-dependent conformational change is required of the 3 M NaCl folded ribozyme that is faster than the rate of ligand binding, we would not observe this event in our catalytic assays. We expect that if such a conformational change exists, however, it is a short-range change in structure to accommodate ligand binding. Nevertheless, the observation that the native *glmS* tertiary structure can form in the complete absence of divalent cations is unique among ribozyme systems. The *Tetrahymena* group I intron ribozyme can be folded to a nearly native three-dimensional conformation at high monovalent cation concentrations[30,43] but requires divalent cations to activate the active site chemistry and to fold the catalytic core. In the case of the *glmS* ribozyme, folding in 3 M NaCl is sufficient to form all hydroxyl radical-protected sites to the same magnitude observed in $MgCl_2$. A high NaCl concentration can mediate native tertiary contacts in the *Schistosoma mansoni* hammerhead ribozyme but does not alone permit efficient catalysis to occur.[27] Furthermore, when molar concentrations are present, the cleavage rate in $MgCl_2$ is reduced 4600-fold, suggesting that monovalent cations are able to compete for divalent cation binding or shield the RNA from divalent cations.[27] In contrast, we find that 3 M NaCl has no observable effect on the ligand-initiated cleavage rate in the presence of 15 mM $MgCl_2$ (Figure 6A). This result indicates that Na^+ is itself capable of folding the RNA to the native conformation but requires the presence of Mg^{2+} ions to activate catalysis. In addition, our data indicate that high salt concentration-induced changes to the electrostatic potential of the RNA do not allow rapid ligand binding and catalysis observed in the presence of Mg^{2+}. $MgCl_2$-mediated reactions in the HDV ribozyme system can be inhibited by up to 10-fold via the addition of high concentrations of monovalent cations, but this inhibition can be partially reversed by increasing the $MgCl_2$ concentration,[44] suggesting that Mg^{2+} ions can preferentially occupy specific binding sites related to catalytic activity. Our results also argue that there is no functional difference between the structure prefolded in $MgCl_2$ or NaCl because both are able to achieve the same cleavage rate enhancement upon addition of GlcN6P and $MgCl_2$. The *T. maritima* lysine riboswitch has also been shown to form nearly identical structures in the presence of K^+ and Mg^{2+} ions.[26]We conclude that folding of the ribozyme is relatively independent of cation identity, but the rapid initiation of catalysis upon the addition of ligand is stricter.

Of the three divalent metals tested, Mg^{2+} was most effective at ~65 min^{-1}, while Ca^{2+} and Mn^{2+} were almost 3-fold slower at ~20 and ~27 min^{-1}, respectively, indicating specific requirements for achieving rapid catalysis. The reduced catalytic rate in the presence of Mn^{2+} and Ca^{2+} could be the result of conformational or structural limitations of the active site. Although Mn^{2+} and Ca^{2+} are the smallest and largest of the divalent cations tested, at 0.67 and 1.12 Å, respectively, they exhibit essentially no difference in their ability to promote catalysis in the presence of ligand. These data may indicate an optimal cation size requirement necessary to effectively position the ligand and promote catalysis.[39] To achieve maximal catalytic activity, it is not unusual for certain ribozymes to discriminate against closely related cations. For example, naturally occurring *Tetrahymena* and *Azoarcus* group I ribozymes exhibit a strong dependence on Mg^{2+} for effective activity and display no detectable activity in vitro with Ca^{2+} as the sole divalent.[45−48] Additionally, the genomic and antigenomic forms of the HDV ribozyme also exhibit an interesting $Mg^{2+}-Ca^{2+}$ switch, in which the genomic form is catalytically efficient in Mg^{2+} whereas the antigenomic form cleaves faster in Ca^{2+}.[49] The difference in rates for the *glmS* ribozyme could also be due to distinct metal ions coordinating GlcN6P in slightly different manners within the ligand-binding pocket, thus promoting a different binding mode that may result in less efficient catalysis.[39]

Finally, altered outer sphere coordination could be responsible for reduced catalytic efficiency when compared to Mg^{2+}. Although all three of the divalent cations tested are hexahydrated, Mg^{2+} strongly prefers an octahedral geometry, while Ca^{2+} is more flexible and has a greater range of coordination numbers and also exhibits a greater range of bond distances.[50] Ca^{2+} and Mn^{2+}, although hexahydrated, may not be able to create or maintain the water-mediated contacts necessary for optimal catalysis, because of the orientation and/or geometry of their surrounding water molecules. Additionally, the coordination geometry and the distance between coordinated ligands may be best suited for Mg^{2+}.[40] $Co(NH_3)_6^{3+}$, a structural mimic of Mg^{2+}, was very inefficient at promoting catalysis in the presence of ligand, with a cleavage rate only slightly above the cleavage rate triggered by ligand and Na^+ alone (Figure 6A). Unlike the associated water ligands of Mg^{2+}, Ca^{2+}, and Mn^{2+}, the ammine ligands of $Co(NH_3)_6^{3+}$ cannot be displaced to make inner sphere contacts.[38] The crystal structure indicates that the Mg^{2+} ions make both outer sphere and water-mediated contacts within the ligand-binding pocket. The ammine groups of $Co(NH_3)_6^{3+}$ should be capable of creating appropriate outer sphere contacts but would be incapable of creating the water-mediated contacts with the nucleobase functional groups within the ligand-binding pocket. These data indicate that to achieve rapid catalysis, there may be a requirement for a specific geometry of water-mediated coordination to achieve appropriate placement of GlcN6P within the binding pocket to promote rapid catalysis. Overall, our data indicate that divalent cations are more effective than monovalent cations or $Co(NH_3)_6^{3+}$ at positioning GlcN6P within the ligand-binding pocket to promote rapid catalysis.

Our evidence supports the hypothesis that this Mg^{2+} or divalent cation requirement is due to the need for divalent cations to bind to GlcN6P and assist in the binding of ligand to the RNA. This hypothesis has been presented previously on the basis of crystallographic structures that model two hydrated Mg^{2+} ions coordinated between RNA functional groups and the phosphate moiety of GlcN6P within the ligand-binding pocket.[12,14] Substitution of glucosamine (GlcN), an analogue of GlcN6P lacking the phosphate group for GlcN6P, eliminates all fast ligand-triggered reaction regardless of the cation employed. All cations tested promote catalysis at a rate of ~2 min^{-1} (Figure 6B), supporting the idea that ligand binding is strongly assisted by divalent cations and that the phosphate moiety of GlcN6P is required for rapid positioning and/or efficient catalytic activity within the ligand-binding pocket (Figure 7). The phosphate group of GlcN6P may help to "lock" the ligand into the ligand-binding pocket. The phosphate edge of the ligand-binding pocket is solvent-exposed. Both Mg^{2+} ions and water molecules act to screen the negative charge of the RNA phosphate backbone from the phosphate group of GlcN6P,[12] while the remaining portion of the ligand is buried within the active site. Glucose 6-phosphate (Glc6P), an analogue of GlcN6P, with a hydroxyl group in place of the primary amine, is a competitive inhibitor of the cleavage reaction.[18] Crystal structures indicate that Glc6P occupies the ligand-binding pocket of the active site in a manner almost identical to that of GlcN6P binding. The *glmS* ribozyme recognizes both the phosphate and sugar moieties of Glc6P,[14] making a set of contacts that is similar to the set made by GlcN6P.[15] Even following cleavage, the *glmS* ribozyme retains affinity for GlcN6P, as postcleavage crystallographic structures identify density for at least the phosphate atom of GlcN6P.[15] Our observation of similar reaction rates in GlcN, where the ligand phosphate is absent, or in the presence of 3 M Na^+ as a sole cation suggests that the same reaction pathway step is limiting. Under all conditions that we have tested, ligand titrations have been conducted, and the reported rates are from experiments in which ligand binding is saturating (see Figures S3 and S4 of the Supporting Information). The intrinsic rate of association of ligand with the ribozyme, however, has not been determined. We do not, therefore, have direct evidence that ligand binding is rate-limiting under these conditions. The flavin mononucleotide (FMN) riboswitch also utilizes a Mg^{2+}-dependent mechanism for coordinating the ligand phosphate in the binding pocket, and biochemical studies have shown a strong preference for binding phosphorylated ligands and the presence of Mg^{2+}.[51] In addition, the glycine riboswitch has been shown to form significant native tertiary structure in the presence of molar concentrations of NaCl but requires specific divalent cations to support ligand binding.[52,53]

Evidence of the importance of the phosphate moiety of GlcN6P with respect to rapid ligand binding has also come from experiments showing that the highest pK_a for a nonbridging phosphate oxygen, as determined by NMR (pH ~6.1), correlates well with the $K_{1/2}$ of the ligand, determined catalytically.[15] The implication is that protonation of a single ligand nonbridging phosphate oxygen impairs ligand binding due to loss of the Mg^{2+} coordination between the ligand and RNA. Thus, the ribozyme is activated under basic conditions. The same conclusion has been reached recently on the basis of molecular dynamics simulations.[54] We determined the pH reactivity profiles determined at saturating concentrations of GlcN6P or GlcN in $MgCl_2$ or 3 M NaCl to examine this idea in greater detail (Figure 7). In both Na^+ and Mg^{2+} GlcN6P-initiated reactions have rate−pH profiles, fit well to a single-ionization equation, and yield pK_a values of 6.4 and 6.5, respectively (Figure 7). This does not fit with the Mg^{2+} requirement in this model but does support the proposal that the nonbridging oxygen can make a hydrogen bond with the N1 hydrogen of the invariant guanosine at position 1, G1, in $MgCl_2$ and 3 M NaCl.[21] Phosphate protonation is expected to both disrupt this interaction and be cation-independent. In

addition, our data are consistent with a model for this rate−pH behavior suggesting a general base role for scissile phosphate *pro-*R_P nonbridging phosphate oxygen.[54]

More recently, molecular dynamics simulations and detailed free energy calculations indicate the apparent pK_a of 6.1 to be attributed to the amine group of GlcN6P.[55] Because both GlcN6P and GlcN retain an amine group at position 2, it is plausible that the apparent pK_a of ∼6.5 cannot be attributed to the phosphate group, but to the amine. To explore this idea further, we determined the pH reactivity profile of the *glmS* ribozyme utilizing saturating concentrations of GlcN in Mg^{2+} or a 3 M NaCl background. Prefolding in $MgCl_2$ followed by GlcN initiation resulted in a 10-fold decrease in the catalytic rate over the pH range tested (pH 5.5−8), fitting to a single ionization event with an apparent pK_a of ∼6.5. We did not observe a pH-dependent cleavage rate when reactions were initiated with 3 M Na^+. It is possible that under these conditions a different, pH-independent, step in the reaction is rate-limiting; however, the rate of GlcN-mediated catalysis is 10-fold faster in the presence of 3 M NaCl than in the presence of $MgCl_2$ at pH 5.5. Another possible reason GlcN is less effective at promoting reaction rates closer to those produced by GlcN6P is the presence of unfilled space within the ligand-binding pocket in the absence of the phosphate group. Without the phosphate moiety to form the fixed network of Mg^{2+}-coordinated interactions with the various functional groups of the ligand-binding pocket, it is possible that the hydrogen bonds coordinating the glucosamine ring are not sufficient to effectively position GlcN for reaction chemistry. In Na^+, the binding pocket may be better able to tolerate protonation of specific residues.

The ligand-initiated site-specific RNA cleavage catalyzed by the *glmS* ribozyme is a very interesting and novel riboswitch mechanism. Ligand recognition is clearly central to the function of all riboswitches, and our data on this topic provide new insight for the glmS ribozyme. We find that both the ligand phosphate moiety and the presence of Mg^{2+} ions make significant contributions to ligand binding and catalysis by the ribozyme. These effects are largely nonadditive, suggesting that they affect the same molecular event. This new insight may be useful in designing chemical agonists or antagonists of the *glmS* ribozyme for the use of antibiotics against Gram-positive bacteria of biomedical importance that employ this catalyst.

■ ASSOCIATED CONTENT

Supporting Information. Hydroxyl radical footprinting of the *glmS* ribozyme 3′ product reveals identical protections in 15 mM $MgCl_2$ and molar concentrations of NaCl (Figure S1). The data presented in Figures S2−S4 show that under all solution conditions employed in these experiments the cation and/or ligand concentrations used were at a level beyond which no increase in catalytic rate is observed. This material is available free of charge via the Internet at http://pubs.acs.org.

■ AUTHOR INFORMATION

Corresponding Author

*E-mail: khampel@uvm.edu. Phone: (802) 656-5852. Fax: (802) 656-8749.

Funding Sources

This work was supported by National Institutes of Health Grant GM065552.

■ ACKNOWLEDGMENT

We thank Dr. John M. Burke and the Department of Microbiology and Molecular Genetics of the University of Vermont for generously supporting this independent line of research and Joyce Heckman for providing helpful discussions.

■ ABBREVIATIONS

EDTA, ethylenediaminetetraacetic acid; FMN, flavin mononucleotide; GlcN, glucosamine; GlcN6P, glucosamine 6-phosphate; HDV, hepatitis delta virus; HEPES, *N*-(2-hydroxyethyl)piperazine-*N*′-(2-ethanesulfonic acid); HPLC, high-performance liquid chromatography; mRNA, messenger ribonucleic acid; PAGE, polyacrylamide gel electrophoresis; PCR, polymerase chain reaction; RNase, ribonuclease; TAPS, *N*-tris(hydroxymethyl)-methyl-3-aminopropanesulfonic acid; TBE, Tris-borate-EDTA; Tris, tris(hydroxymethyl)aminomethane; tRNA, transfer ribonucleic acid; UV, ultraviolet; VS, Varkud satellite.

■ REFERENCES

(1) Winkler, W. C., and Breaker, R. R. (2005) Regulation of bacterial gene expression by riboswitches. *Annu. Rev. Microbiol. 59*, 487–517.

(2) Winkler, W., Nahvi, A., and Breaker, R. R. (2002) Thiamine derivatives bind messenger RNAs directly to regulate bacterial gene expression. *Nature 419*, 952–956.

(3) Mironov, A. S., Gusarov, I., Rafikov, R., Lopez, L. E., Shatalin, K., Kreneva, R. A., Perumov, D. A., and Nudler, E. (2002) Sensing small molecules by nascent RNA: A mechanism to control transcription in bacteria. *Cell 111*, 747–756.

(4) Nudler, E., and Mironov, A. S. (2004) The riboswitch control of bacterial metabolism. *Trends Biochem. Sci. 29*, 11–17.

(5) Barrick, J. E., Corbino, K. A., Winkler, W. C., Nahvi, A., Mandal, M., Collins, J., Lee, M., Roth, A., Sudarsan, N., Jona, I., Wickiser, J. K., and Breaker, R. R. (2004) New RNA motifs suggest an expanded scope for riboswitches in bacterial genetic control. *Proc. Natl. Acad. Sci. U.S.A. 101*, 6421–6426.

(6) Winkler, W. C., Nahvi, A., Roth, A., Collins, J. A., and Breaker, R. R. (2004) Control of gene expression by a natural metabolite-responsive ribozyme. *Nature 428*, 281–286.

(7) Kobayashi, K., Ehrlich, S. D., Albertini, A., Amati, G., Andersen, K. K., Arnaud, M., Asai, K., Ashikaga, S., Aymerich, S., Bessieres, P., Boland, F., Brignell, S. C., Bron, S., Bunai, K., Chapuis, J., Christiansen, L. C., Danchin, A., Debarbouille, M., Dervyn, E., Deuerling, E., Devine, K., Devine, S. K., Dreesen, O., Errington, J., Fillinger, S., Foster, S. J., Fujita, Y., Galizzi, A., Gardan, R., Eschevins, C., Fukushima, T., Haga, K., Harwood, C. R., Hecker, M., Hosoya, D., Hullo, M. F., Kakeshita, H., Karamata, D., Kasahara, Y., Kawamura, F., Koga, K., Koski, P., Kuwana, R., Imamura, D., Ishimaru, M., Ishikawa, S., Ishio, I., Le Coq, D., Masson, A., Mauel, C., Meima, R., Mellado, R. P., Moir, A., Moriya, S., Nagakawa, E., Nanamiya, H., Nakai, S., Nygaard, P., Ogura, M., Ohanan, T., O'Reilly, M., O'Rourke, M., Pragai, Z., Pooley, H. M., Rapoport, G., Rawlins, J. P., Rivas, L. A., Rivolta, C., Sadaie, A., Sadaie, Y., Sarvas, M., Sato, T., Saxild, H. H., Scanlan, E., Schumann, W., Seegers, J. F., Sekiguchi, J., Sekowska, A., Seror, S. J., Simon, M., Stragier, P., Studer, R., Takamatsu, H., Tanaka, T., Takeuchi, M., Thomaides, H. B., Vagner, V., van Dijl, J. M., Watabe, K., Wipat, A., Yamamoto, H., Yamamoto, M., Yamamoto, Y., Yamane, K., Yata, K., Yoshida, K., Yoshikawa, H., Zuber, U., and Ogasawara, N. (2003) Essential *Bacillus subtilis* genes. *Proc. Natl. Acad. Sci. U.S.A. 100*, 4678–4683.

(8) Milewski, S. (2002) Glucosamine-6-phosphate synthase: The multi-facets enzyme. *Biochim. Biophys. Acta 1597*, 173–192.

(9) Collins, J. A., Irnov, I., Baker, S., and Winkler, W. C. (2007) Mechanism of mRNA destabilization by the glmS ribozyme. *Genes Dev. 21*, 3356–3368.

(10) Komatsuzawa, H., Fujiwara, T., Nishi, H., Yamada, S., Ohara, M., McCallum, N., Berger-Bachi, B., and Sugai, M. (2004) The gate

controlling cell wall synthesis in *Staphylococcus aureus*. *Mol. Microbiol. 53*, 1221–1231.

(11) Tinsley, R. A., Furchak, J. R., and Walter, N. G. (2007) Trans-acting glmS catalytic riboswitch: Locked and loaded. *RNA 13*, 468–477.

(12) Cochrane, J. C., Lipchock, S. V., and Strobel, S. A. (2007) Structural investigation of the GlmS ribozyme bound to its catalytic cofactor. *Chem. Biol. 14*, 97–105.

(13) Hampel, K. J., and Tinsley, M. M. (2006) Evidence for preorganization of the glmS ribozyme ligand binding pocket. *Biochemistry 45*, 7861–7871.

(14) Klein, D. J., and Ferré-D'Amaré, A. R. (2006) Structural basis of *glmS* ribozyme activation by glucosamine-6-phosphate. *Science 313*, 1752–1756.

(15) Cochrane, J. C., Lipchock, S. V., Smith, K. D., and Strobel, S. A. (2009) Structural and chemical basis for glucosamine 6-phosphate binding and activation of the glmS ribozyme. *Biochemistry 48*, 3239–3246.

(16) Brooks, K. M., and Hampel, K. J. (2009) A rate-limiting conformational step in the catalytic pathway of the glmS ribozyme. *Biochemistry 48*, 5669–5678.

(17) Roth, A., Nahvi, A., Lee, M., Jona, I., and Breaker, R. R. (2006) Characteristics of the glmS ribozyme suggest only structural roles for divalent metal ions. *RNA 12*, 607–619.

(18) McCarthy, T. J., Plog, M. A., Floy, S. A., Jansen, J. A., Soukup, J. K., and Soukup, G. A. (2005) Ligand requirements for glmS ribozyme self-cleavage. *Chem. Biol. 12*, 1221–1226.

(19) Cochrane, J. C., and Strobel, S. A. (2008) Riboswitch effectors as protein enzyme cofactors. *RNA 14*, 993–1002.

(20) Jansen, J. A., McCarthy, T. J., Soukup, G. A., and Soukup, J. K. (2006) Backbone and nucleobase contacts to glucosamine-6-phosphate in the glmS ribozyme. *Nat. Struct. Mol. Biol. 13*, 517–523.

(21) Klein, D. J., Wilkinson, S. R., Been, M. D., and Ferre-D'Amare, A. R. (2007) Requirement of helix P2.2 and nucleotide G1 for positioning the cleavage site and cofactor of the glmS ribozyme. *J. Mol. Biol. 373*, 178–189.

(22) DeRose, V. J. (2003) Metal ion binding to catalytic RNA molecules. *Curr. Opin. Struct. Biol. 13*, 317–324.

(23) Draper, D. E. (2004) A guide to ions and RNA structure. *RNA 10*, 335–343.

(24) Murray, J. B., Seyhan, A. A., Walter, N. G., Burke, J. M., and Scott, W. G. (1998) The hammerhead, hairpin and VS ribozymes are catalytically proficient in monovalent cations alone. *Chem. Biol. 5*, 587–595.

(25) Nesbitt, S., Hegg, L. A., and Fedor, M. J. (1997) An unusual pH-independent and metal-ion-independent mechanism for hairpin ribozyme catalysis. *Chem. Biol. 4*, 619–630.

(26) Serganov, A., Huang, L., and Patel, D. J. (2008) Structural insights into amino acid binding and gene control by a lysine riboswitch. *Nature 455*, 1263–1267.

(27) Boots, J. L., Canny, M. D., Azimi, E., and Pardi, A. (2008) Metal ion specificities for folding and cleavage activity in the *Schistosoma* hammerhead ribozyme. *RNA 14*, 2212–2222.

(28) Ke, A., Ding, F., Batchelor, J. D., and Doudna, J. A. (2007) Structural roles of monovalent cations in the HDV ribozyme. *Structure 15*, 281–287.

(29) Krasovska, M. V., Sefcikova, J., Reblova, K., Schneider, B., Walter, N. G., and Sponer, J. (2006) Cations and hydration in catalytic RNA: Molecular dynamics of the hepatitis delta virus ribozyme. *Biophys. J. 91*, 626–638.

(30) Travers, K. J., Boyd, N., and Herschlag, D. (2007) Low specificity of metal ion binding in the metal ion core of a folded RNA. *RNA 13*, 1205–1213.

(31) Gordon, P. M., Sontheimer, E. J., and Piccirilli, J. A. (2000) Kinetic characterization of the second step of group II intron splicing: role of metal ions and the cleavage site 2′-OH in catalysis. *Biochemistry 39*, 12939–12952.

(32) Shan, S., Yoshida, A., Sun, S., Piccirilli, J. A., and Herschlag, D. (1999) Three metal ions at the active site of the *Tetrahymena* group I ribozyme. *Proc. Natl. Acad. Sci. U.S.A. 96*, 12299–12304.

(33) Shan, S. O., and Herschlag, D. (1999) Probing the role of metal ions in RNA catalysis: Kinetic and thermodynamic characterization of a metal ion interaction with the 2′-moiety of the guanosine nucleophile in the *Tetrahymena* group I ribozyme. *Biochemistry 38*, 10958–10975.

(34) Takamoto, K., He, Q., Morris, S., Chance, M. R., and Brenowitz, M. (2002) Monovalent cations mediate formation of native tertiary structure of the *Tetrahymena thermophila* ribozyme. *Nat. Struct. Biol. 9*, 928–933.

(35) Klawuhn, K., Jansen, J. A., Souchek, J., Soukup, G. A., and Soukup, J. K. (2010) Analysis of metal ion dependence in glmS ribozyme self-cleavage and coenzyme binding. *ChemBioChem 11*, 2567–2571.

(36) Walter, N. G., Yang, N., and Burke, J. M. (2000) Probing non-selective cation binding in the hairpin ribozyme with Tb(III). *J. Mol. Biol. 298*, 539–555.

(37) Chowrira, B. M., Berzal-Herranz, A., and Burke, J. M. (1993) Novel RNA polymerization reaction catalyzed by a group I ribozyme. *EMBO J. 12*, 3599–3605.

(38) Cowan, J. A. (1993) Metallobiochemistry of RNA. $Co(NH_3)_6^{3+}$ as a probe for $Mg^{2+}(aq)$ binding sites. *J. Inorg. Biochem. 49*, 171–175.

(39) Schnabl, J., and Sigel, R. K. (2010) Controlling ribozyme activity by metal ions. *Curr. Opin. Chem. Biol. 14*, 269–275.

(40) Woodson, S. A. (2005) Metal ions and RNA folding: A highly charged topic with a dynamic future. *Curr. Opin. Chem. Biol. 9*, 104–109.

(41) Lambert, D., and Draper, D. E. (2007) Effects of osmolytes on RNA secondary and tertiary structure stabilities and RNA-Mg^{2+} interactions. *J. Mol. Biol. 370*, 993–1005.

(42) Basu, S., Rambo, R. P., Strauss-Soukup, J., Cate, J. H., Ferre-D'Amare, A. R., Strobel, S. A., and Doudna, J. A. (1998) A specific monovalent metal ion integral to the AA platform of the RNA tetraloop receptor. *Nat. Struct. Biol. 5*, 986–992.

(43) Takamoto, K., Das, R., He, Q., Doniach, S., Brenowitz, M., Herschlag, D., and Chance, M. R. (2004) Principles of RNA compaction: Insights from the equilibrium folding pathway of the P4-P6 RNA domain in monovalent cations. *J. Mol. Biol. 343*, 1195–1206.

(44) Perrotta, A. T., and Been, M. D. (2006) HDV ribozyme activity in monovalent cations. *Biochemistry 45*, 11357–11365.

(45) Celander, D. W., and Cech, T. R. (1991) Visualizing the higher order folding of a catalytic RNA molecule. *Science 251*, 401–407.

(46) Grosshans, C. A., and Cech, T. R. (1989) Metal ion requirements for sequence-specific endoribonuclease activity of the *Tetrahymena* ribozyme. *Biochemistry 28*, 6888–6894.

(47) McConnell, T. S., Herschlag, D., and Cech, T. R. (1997) Effects of divalent metal ions on individual steps of the *Tetrahymena* ribozyme reaction. *Biochemistry 36*, 8293–8303.

(48) Cernak, P., Madix, R. A., Kuo, L. Y., and Lehman, N. (2008) Accommodation of Ca(II) ions for catalytic activity by a group I ribozyme. *J. Inorg. Biochem. 102*, 1495–1506.

(49) Perrotta, A. T., and Been, M. D. (2007) A single nucleotide linked to a switch in metal ion reactivity preference in the HDV ribozymes. *Biochemistry 46*, 5124–5130.

(50) Moncrief, M. B., and Maguire, M. E. (1999) Magnesium transport in prokaryotes. *J. Biol. Inorg. Chem. 4*, 523–527.

(51) Serganov, A., Huang, L., and Patel, D. J. (2009) Coenzyme recognition and gene regulation by a flavin mononucleotide riboswitch. *Nature 458*, 233–237.

(52) Lipfert, J., Sim, A. Y., Herschlag, D., and Doniach, S. (2010) Dissecting electrostatic screening, specific ion binding, and ligand binding in an energetic model for glycine riboswitch folding. *RNA 16*, 708–719.

(53) Huang, L., Serganov, A., and Patel, D. J. (2010) Structural insights into ligand recognition by a sensing domain of the cooperative glycine riboswitch. *Mol. Cell 40*, 774–786.

(54) Banas, P., Walter, N. G., Sponer, J., and Otyepka, M. (2010) Protonation states of the key active site residues and structural dynamics of the glmS riboswitch as revealed by molecular dynamics. *J. Phys. Chem. B 114*, 8701–8712.

(55) Xin, Y., and Hamelberg, D. (2010) Deciphering the role of glucosamine-6-phosphate in the riboswitch action of glmS ribozyme. *RNA 16*, 2455–2463.